Shock tube measurements of the rate constants for seven large alkanes + OH

ARTICLE *in* PROCEEDINGS OF THE COMBUSTION INSTITUTE · JUNE 2014

Impact Factor: 2.26 · DOI: 10.1016/j.proci.2014.05.098

ARTICLE IN PRESS

Available online at www.sciencedirect.com

ScienceDirect

Proceedings of the Combustion Institute xxx (2014) xxx–xxx

Proceedings of the Combustion Institute

www.elsevier.com/locate/proci

Shock tube measurements of the rate constants for seven large alkanes + OH

Jihad Badra, Ahmed Elwardany, Aamir Farooq *

Clean Combustion Research Center, Division of Physical Sciences and Engineering, King Abdullah University of Science and Technology (KAUST), Thuwal 23955, Saudi Arabia

Abstract

Reaction rate constants for seven large alkanes + hydroxyl (OH) radicals were measured behind reflected shock waves using OH laser absorption. The alkanes, n-hexane, 2-methyl-pentane, 3-methyl-pentane, 2,2-dimethyl-butane, 2,3-dimethyl-butane, 2-methyl-heptane, and 4-methyl-heptane, were selected to investigate the rates of site-specific H-abstraction by OH at secondary and tertiary carbons. Hydroxyl radicals were monitored using narrow-line-width ring-dye laser absorption of the $R_1(5)$ transition of the OH spectrum near 306.7 nm. The high sensitivity of the diagnostic enabled the use of low reactant concentrations and pseudo-first-order kinetics. Rate constants were measured at temperatures ranging from 880 K to 1440 K and pressures near 1.5 atm. High-temperature measurements of the rate constants for OH + n-hexane and OH + 2,2-dimethyl-butane are in agreement with earlier studies, and the rate constants of the five other alkanes with OH, we believe, are the first direct measurements at combustion temperatures. Using these measurements and the site-specific H-abstraction measurements of Sivaramakrishnan and Michael (2009) [1,2], general expressions for three secondary and two tertiary abstraction rates were determined as follows (the subscripts indicate the number of carbon atoms bonded to the next-nearest-neighbor carbon):

$$S_{20} = 1.58 \times 10^{-11}\exp(-1550\ \mathrm{K/T})\ \mathrm{cm^3\ molecule^{-1}\ s^{-1}}\ (887\text{–}1327\ \mathrm{K})$$
$$S_{30} = 2.37 \times 10^{-11}\exp(-1850\ \mathrm{K/T})\ \mathrm{cm^3\ molecule^{-1}\ s^{-1}}\ (887\text{–}1327\ \mathrm{K})$$
$$S_{21} = 4.5 \times 10^{-12}\exp(-793.7\ \mathrm{K/T})\ \mathrm{cm^3\ molecule^{-1}\ s^{-1}}\ (833\text{–}1440\ \mathrm{K})$$
$$T_{100} = 2.85 \times 10^{-11}\exp(-1138.3\ \mathrm{K/T})\ \mathrm{cm^3\ molecule^{-1}\ s^{-1}}\ (878\text{–}1375\ \mathrm{K})$$
$$T_{101} = 7.16 \times 10^{-12}\exp(-993\ \mathrm{K/T})\ \mathrm{cm^3\ molecule^{-1}\ s^{-1}}\ (883\text{–}1362\ \mathrm{K})$$

Keywords: Alkanes; Hydroxyl radicals; Rate constants; Shock tube; Site-specific rates

* Corresponding author. Tel.: +966 128082704.
E-mail address: aamir.farooq@kaust.edu.sa (A. Farooq).

http://dx.doi.org/10.1016/j.proci.2014.05.098
1540-7489/

Please cite this article in press as: J. Badra et al., *Proc. Combust. Inst.* (2014), http://dx.doi.org/10.1016/j.proci.2014.05.098

1. Introduction

The reactions of alkanes, both normal and branched, with the hydroxyl radical OH are the primary oxidation routes for these fuel components at combustion conditions [3,4]. These reactions are important because small normal and branched alkanes ($<C_5$) make up almost all of the composition of natural and liquefied petroleum gas (LPG), and the larger straight-chain and branched alkanes ($\geqslant C_5$) are primary constituents of gasoline, diesel, and aviation fuels [5–7]. Despite the significant importance of these reactions, there is a lack of direct rate constant measurements for OH with large alkanes, particularly at high temperatures.

Though there are only a limited number of studies of large alkanes + OH, there is an active literature in this area. Atkinson [3,8–11] periodically reviewed the low and high-temperature gas-phase reaction rate constants of OH radicals with various alkanes. At temperatures below 900 K, Tully and co-workers [12–17] studied the reaction rate of OH with various alkanes to determine the site-specific (primary, secondary, and tertiary) rate constants of H- and D-abstraction by OH radical. This work was complemented by single-point high temperature (1100–1200 K) measurements performed by Cohen and co-workers [4,18–21]. Sivaramakrishnan and Michael [1,2] measured the reaction rate constants of OH with a few normal and branched alkanes at high temperatures (797–1259 K). As well, Pang et al. [22] measured the rate constants of n-pentane, n-heptane, and n-nonane with OH at temperatures ranging from 869 to 1364 K. Because of the significant curvature exhibited by the rate constants at high temperatures, as shown in [4,12–21], further direct measurements are needed.

There have been some efforts to develop rate estimation methods to describe the non-Arrhenius behavior of the Fuel + OH rate and to predict rate constants for fuels where experimental data are not available. Cohen [23,24] used the group-additivity transition-state-theory (TST) method to reproduce their single-temperature measurements [4,18–21]. Atkinson and co-workers [8,25] developed another estimation method, known as the structure–reactivity approach (SAR), to predict the reactivity of OH with various alkanes and oxygenated molecules. Recently, Sivaramakrishnan and Michael [1,2] extended the next-nearest-neighbor (N-N-N) estimation method of Cohen [23,24] to determine several site-specific H abstraction rate constants over a wide temperature range. Their derived rates satisfactorily reproduce the experimentally measured rate constants of OH with many alkanes including the heavier molecules such as n-hexadecane. However, their site-specific rate constant expressions cannot be employed to all normal and branched alkanes because a few important site-specific rate constant expressions are not available from their work. This deficiency can be overcome by obtaining new experimental data for carefully-chosen molecules to derive additional site-specific rates.

Here, we report the rate constant measurements of the reaction of seven different alkanes with OH:

$$\text{n-hexane} + OH \rightarrow C_6H_{13}\text{-}1 + H_2O \quad (R1)$$

$$\text{2-methyl-pentane} + OH \rightarrow C_6H_{13}\text{-}2 + H_2O \quad (R2)$$

$$\text{3-methyl-pentane} + OH \rightarrow C_6H_{13}\text{-}3 + H_2O \quad (R3)$$

$$\text{2,2-dimethyl-butane} + OH \rightarrow C_6H_{13}\text{-}2\text{-}2 + H_2O \quad (R4)$$

$$\text{2,3-dimethyl-butane} + OH \rightarrow C_6H_{13}\text{-}2\text{-}3 + H_2O \quad (R5)$$

$$\text{2-methyl-heptane} + OH \rightarrow C_8H_{17}\text{-}2 + H_2O \quad (R6)$$

$$\text{4-methyl-heptane} + OH \rightarrow C_8H_{17}\text{-}4 + H_2O \quad (R7)$$

New site-specific rate constants for the H abstraction by OH from secondary and tertiary H atoms are derived from these measurements and the effects of methyl (CH_3) branching and location of CH_3 on the reaction rate constants of OH with alkanes are examined.

2. Experimental methods

The current experiments were performed in the stainless steel, high-purity, low-pressure shock tube (LPST) facility at King Abdullah University of Science and Technology (KAUST). The method and setup were detailed previously [26,27] and only a brief description is given here. The shock tube is made of a 9 m driver section and a 9 m driven section, with an inner diameter of 14.2 cm. The incident shock speed is measured using a series of five piezoelectric PCB pressure transducers over the last 1.3 m of the shock tube. Reflected shock temperatures and pressures are determined from the measured incident shock speed and standard shock-jump relations. Uncertainties in the calculated temperatures and pressures are approximately ±0.7% and ±1%, respectively, mainly due to the uncertainty in the measured shock velocity (±0.2%). The facility is equipped with a magnetically-stirred 24 L mixing vessel and a well-furnished mixing manifold for the accurate preparation of mixtures. The OH laser diagnostic and a Kistler 603B piezoelectric pressure transducer are located at a test section 2 cm from the driven section endwall.

The ultraviolet light for OH absorption is generated by the external frequency doubling of red light (614 nm) produced by a ring-dye cw laser (from Sirah) pumped by a 10 W green laser. This system delivers about 100 mW of cw light in the UV. In the current experiments, the UV laser wavelength is tuned to the center (306.6868 nm) of the well-characterized $R_1(5)$ absorption line in

Please cite this article in press as: J. Badra et al., *Proc. Combust. Inst.* (2014), http://dx.doi.org/10.1016/j.proci.2014.05.098

the OH A–X (0, 0) absorption band. A common-mode-rejection scheme is used here which gives a detection limit of about 0.2 ppm at 1400 K and 1 atm, assuming a minimum detectable absorbance of 0.1%. The OH mole fraction is calculated from Beer's law, $I/I_o = \exp(-k_{OH}X_{OH}PL)$, where I and I_o are the transmitted and incident laser intensities, k_{OH} is the OH absorption coefficient, X_{OH} is the OH mole fraction, P is the total pressure (atm), and L is the path length (14.2 cm). The overall estimated uncertainty in the measured OH mole fraction (X_{OH}) is approximately ±3%, mainly due to the uncertainty in temperature and available absorption cross-section data [28]. Experimental data are recorded at a sampling rate of 2.5 MHz using a high-resolution (14 bit) data acquisition system (National Instruments).

Hydroxyl radicals were produced by rapid thermal decomposition of tert-butyl hydroperoxide (TBHP), where TBHP is known to be a clean OH precursor and has been validated in many studies [22,26,29–35]. A 70% TBHP in water solution, n-hexane (⩾98%), 2-methyl-pentane (⩾99%), 3-methyl-pentane (⩾99%), 2,2-dimethyl-butane (⩾99%), 2,3-dimethyl-butane (⩾98%), 2-methyl-heptane (⩾98%) were obtained from ChemSampCo., and 4-methyl-heptane (⩾99%) was purchased from Sigma Aldrich. Further purification is performed on all alkanes by utilizing the freeze–pump-thaw method. A double-dilution process was utilized when preparing mixtures to obtain accurate concentrations in the mixing tank [29].

Chemkin-Pro [36] commercial software was used to perform zero-dimensional simulations with constant internal energy and volume (constant UV) constraints. Of the fuels studied in this work, only n-hexane and 2-methyl-heptane have previously published detailed mechanisms [37] which were used to fit the experimental data for deducing fuel + OH rates. For the other five fuels, sub-mechanisms comprising of fuel + OH reactions and the decomposition reactions of the various fuel fragments are developed in this work, as will be explained later. In addition to the original base mechanism and the sub-mechanisms for fuel + OH, a sub-mechanism describing the decomposition of TBHP and its subsequent radicals was added from [26]. The experiments were designed to have relatively larger fuel concentrations (128–204 ppm in argon) so that the removal of OH (initially at 10–20 ppm) was controlled by pseudo-first-order kinetics.

3. Results and discussion

3.1. High temperature measurements of Fuel + OH → Products

The rate constant of n-hexane + OH → Products, was measured using a mixture of 200 ppm of n-hexane, 11 ppm of TBHP (30 ppm of water) balance Ar that was shock-heated to post-shock temperatures of 881–1351 K at 1.5 atm. An OH sensitivity analysis confirmed that this mixture composition provided good isolation of the target reaction. Here, normalized OH sensitivity is defined as, $S_{OH} = (\partial X_{OH}/\partial k_i) \times (k_i/X_{OH})/S_{OH,Max}$, where X_{OH} is the local OH mole fraction and k_i is the rate constant of the ith reaction. A representative OH sensitivity is plotted in Fig. 1 and shows that n-hexane + OH is the dominant reaction. However, minor interferences from secondary reactions do occur and the rates for the important secondary reactions are updated based on the values given in [26]. The reaction n-hexane + OH has three different pathways:

$$\text{n-}C_6H_{14} + OH \rightarrow C_6H_{13}\text{-}1 + H_2O \quad \text{(R1a)}$$

$$\text{n-}C_6H_{14} + OH \rightarrow C_6H_{13}\text{-}2 + H_2O \quad \text{(R1b)}$$

$$\text{n-}C_6H_{14} + OH \rightarrow C_6H_{13}\text{-}3 + H_2O \quad \text{(R1c)}$$

The branching ratios ($k_{1a or 1b or 1c}/k_{total}$) for these reactions [37] at 1033 K are 0.24 for R1a (primary) and 0.38 for both R1b (secondary) and R1c (secondary). These branching ratios were kept unchanged when fitting the experimental profiles, but separate modeling shows that the determination of overall rate constant ($k_1 = k_{1a} + k_{1b} + k_{1c}$) was effectively insensitive to the branching ratios values. Fig. 2 shows a representative raw trace of the measured OH time-history at 1033 K and 1.56 atm. The initial TBHP concentration in the simulations is taken from the experimental OH yield. Note that the experimental slow rise of OH before $t = 0$ is attributed to the relatively low bandwidth (760 kHz) of the detector. The detector bandwidth can be set as high as 10 GHz but the signal to noise ratio is quite low

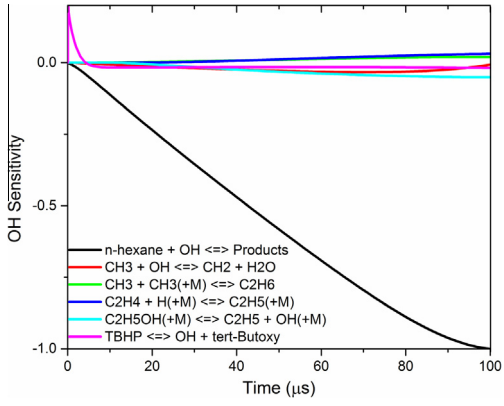

Fig. 1. OH sensitivity for the rate constant measurement of n-hexane + OH at 1033 K and 1.56 atm. Mixture: 200 ppm n-hexane, 11 ppm TBHP (30 ppm H_2O), balance Ar.

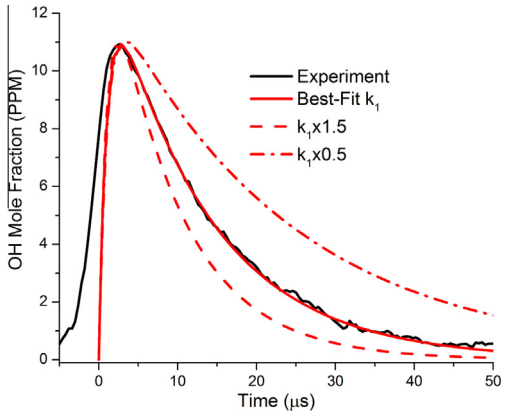

Fig. 2. n-hexane + OH reaction rate measurement for the experimental conditions of Fig. 1. The best fit from the simulations as well as perturbations of ±50% are also presented.

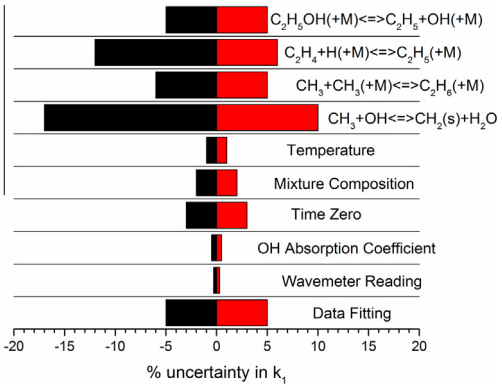

Fig. 3. Uncertainty analysis for the rate constant of n-hexane + OH ⇒ products at 1033 K and 1.56 atm.

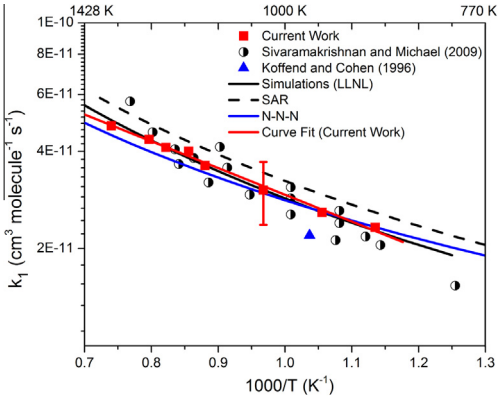

Fig. 4. Arrhenius plot of n-hexane + OH ⇒ products.

at high bandwidths. The problem of slow OH rise occurs only at high temperatures where the decomposition of TBHP is almost instantaneous. However, at lower temperatures (<1150 K) this problem disappears because the used detector bandwidth is high enough to capture the rise of OH fairly well. The best-fit OH profile has a k_1 value of 3.04×10^{-11} cm^3 molecule^{-1} s^{-1} and the effect of 50% deviations from this value is also presented in Fig. 2.

A detailed sensitivity analysis was performed to estimate the errors in the measured rate constants for R1 at 1033 K and 1.56 atm. The various sources of errors considered here include the temperature (±0.7%), the mixture composition (±5%), the OH absorption coefficient (±3%), the wavemeter reading (±0.002 cm^{-1}), errors in fitting the experimental profile (±5%), locating time zero (±0.5 μs), and the rate constants of the secondary reactions. The contribution of each of these error sources on the determination of k_1 is calculated separately and presented in Fig. 3. The overall uncertainty is calculated using the root-sum-squared method and is found to be ±22% for k_1 at 1033 K.

The Arrhenius plot of the rate constant of n-hexane + OH ⇒ products is shown in Fig. 4 as are the values calculated using two estimation methods (SAR and N-N-N). The experimental data agree with the previously published data by Sivaramakrishnan and Michael [1] though our data have considerably less scatter. The rates used in the Sarathy et al. mechanism [37] also agree very well with the measurement.

Similar procedures were used to measure the reaction rate constants of fuel + OH for the other six alkanes. Fuel concentrations ranged from 200 to 208 ppm except for 2-methyl-heptane and 4-methyl-heptane which have relatively faster rate constants and smaller fuel concentrations of 128 ppm and 141 ppm were used for 2-methyl-heptane and 4-methyl-heptane, respectively. Experiments were carried out over a range of temperatures for each fuel and the experimental data were fit using either an existing mechanism (2-methyl-heptane) or sub-mechanism developed here. An example of a developed sub-mechanism is given here for 2-methyl-pentane. The reaction rates of OH with 2-methyl-pentane are assumed to be similar to OH + 2-methyl-hexane which are available in Sarathy's et al. mechanism [37]. There are five channels for 2-methyl-pentane + OH reaction:

$$C_6H_{14}\text{-}2 + OH \rightarrow C_6H_{13}\text{-}2a + H_2O \quad (R2a)$$
$$C_6H_{14}\text{-}2 + OH \rightarrow C_6H_{13}\text{-}2b + H_2O \quad (R2b)$$
$$C_6H_{14}\text{-}2 + OH \rightarrow C_6H_{13}\text{-}2c + H_2O \quad (R2c)$$
$$C_6H_{14}\text{-}2 + OH \rightarrow C_6H_{13}\text{-}2d + H_2O \quad (R2d)$$
$$C_6H_{14}\text{-}2 + OH \rightarrow C_6H_{13}\text{-}2e + H_2O \quad (R2e)$$

The rates for these five channels are similar to the rates for 2-methyl-hexane + OH due to the similar structure of the two molecules. So the rates

Please cite this article in press as: J. Badra et al., *Proc. Combust. Inst.* (2014), http://dx.doi.org/10.1016/j.proci.2014.05.098

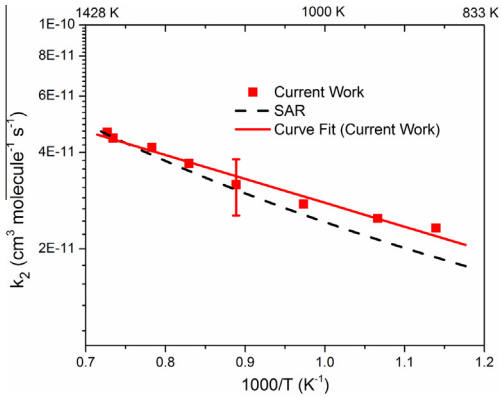

Fig. 5. Arrhenius plot of 2-methyl-pentane + OH ⇒ products.

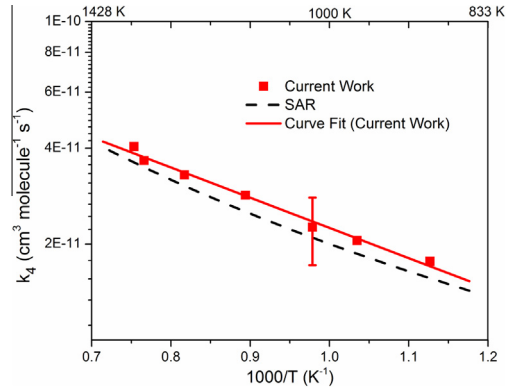

Fig. 7. Arrhenius plot of 2,2-dimethyl-butane + OH ⇒ products.

of channels a, b, and c in 2-methyl-penatne system are similar to the rates of channels a, b, and c in 2-methyl-hexane. Channels d and e in 2-methyl-pentane are similar to channels e and f in 2-methyl-hexane, respectively. Additionally, it is assumed that the various products (C_6H_{13}-2a, b, c, d, and e) decompose similar to the products of 2-methyl-hexane + OH (C_7H_{15}-2a, b, c, d, e, and f) described in Sarathy et al. mechanism [37]. Similar methodology is followed for the rest of molecules where detailed kinetic mechanisms are not available. Again these estimates of the branching ratios are not expected to affect the pseudo-first-order derived overall reaction rate constants. The proposed sub-mechanisms for the five alkanes (2-methyl-pentane, 3-methyl-pentane, 2,2-dimethyl-butane, 2,3-dimethyl-butane, and 4-methyl-heptane) are given in Tables S2-S6 (Supplementary Material). Also, a schematic of each molecule highlighting the nomenclature of H atoms (a, b, c, d, and e) is shown for each molecule under its reaction rate table in the

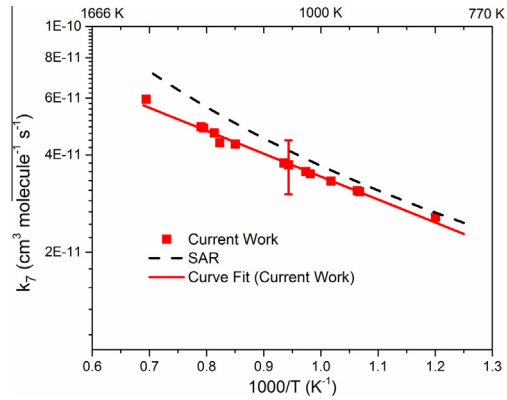

Fig. 8. Arrhenius plot of 4-methyl-heptane + OH ⇒ products.

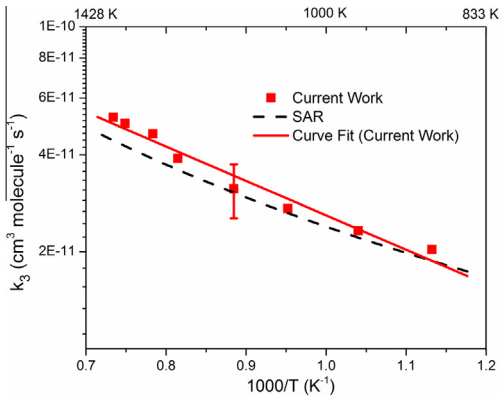

Fig. 6. Arrhenius plot of 3-methyl-pentane + OH ⇒ products.

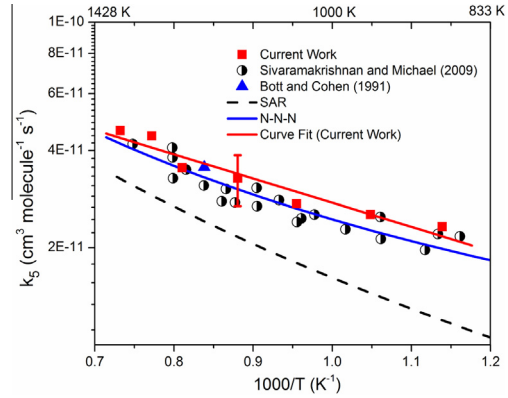

Fig. 9. Arrhenius plot of 2,3-dimethyl-butane + OH ⇒ products.

Supplementary Material. The measured rate constants for 2-methyl-pentane (k_2), 3-methyl-pentane (k_3), 2,2-dimethyl-butane (k_4), and 4-methyl-heptane (k_7) are presented in Figs. 5–8 and compared with the SAR estimation method. Generally, the SAR method under-predicts the rate constants considerably except for 4-methyl-heptane where SAR estimation is larger by a factor of 2 or more.

In addition to n-hexane, only 2,3-dimethyl-butane reaction with OH has previously been investigated at high temperatures. Therefore, the current measured are compared with previous studies in Fig. 9. Our data are in good agreement with the measurements of Sivaramakrishnan and Michael [1], though our data have less scatter. Also, the single-temperature measurement by Bott and Cohen [4] agrees well with our measurements. The Arrhenius expressions (the "curve fits" shown in the figures) for the rate constants of the seven alkanes with OH at the studied temperature range are listed below. Estimated errors derived from detailed uncertainty analyses are also given at a specific temperature.

$$k_1 = 1.98 \times 10^{-10}\exp(-1909\ \mathrm{K/T})\ \mathrm{cm^3\ molecule^{-1}\ s^{-1}}\ (881\text{–}1351\ \mathrm{K}), \pm 23\%\ at\ 1033\ \mathrm{K} \quad (1)$$

$$k_2 = 1.55 \times 10^{-10}\exp(-1716\ \mathrm{K/T})\ \mathrm{cm^3\ molecule^{-1}\ s^{-1}}\ (878\text{–}1362\ \mathrm{K}), \pm 20\%\ at\ 1125\ \mathrm{K} \quad (2)$$

$$k_3 = 3.05 \times 10^{-10}\exp(-2464\ \mathrm{K/T})\ \mathrm{cm^3\ molecule^{-1}\ s^{-1}}\ (883\text{–}1362\ \mathrm{K}), \pm 19\%\ at\ 1130\ \mathrm{K} \quad (3)$$

$$k_4 = 2.00 \times 10^{-10}\exp(-2185\ \mathrm{K/T})\ \mathrm{cm^3\ molecule^{-1}\ s^{-1}}\ (887\text{–}1327\ \mathrm{K}), \pm 24\%\ at\ 1021\ \mathrm{K} \quad (4)$$

$$k_5 = 1.55 \times 10^{-10}\exp(-1727\ \mathrm{K/T})\ \mathrm{cm^3\ molecule^{-1}\ s^{-1}}\ (878\text{–}1366\ \mathrm{K}), \pm 18\%\ at\ 1135\ \mathrm{K} \quad (5)$$

$$k_6 = 1.89 \times 10^{-10}\exp(-1624\ \mathrm{K/T})\ \mathrm{cm^3\ molecule^{-1}\ s^{-1}}\ (914\text{–}1405\ \mathrm{K}), \pm 23\%\ at\ 1022\ \mathrm{K} \quad (6)$$

$$k_7 = 1.76 \times 10^{-10}\exp(-1635\ \mathrm{K/T})\ \mathrm{cm^3\ molecule^{-1}\ s^{-1}}\ (833\text{–}1440\ \mathrm{K}), \pm 19\%at\ 1060\ \mathrm{K} \quad (7)$$

3.2. Secondary and tertiary H-abstraction rate constants

Several theoretical methods are available to calculate the rate constants of alkanes with OH in the absence of experimental data. As discussed earlier, these estimations include the SAR method of Atkinson and co-workers [8,25] and the N-N-N method of Sivaramakrishnan and Michael [1,2]. The N-N-N (next-nearest-neighbor) designation is based on the understanding that the primary, secondary, and tertiary C-H bonds are dependent on the number of C atoms bonded to the N-N-N carbon atom. For the current work, the N-N-N estimation method can be used to calculate the rate constants of the reaction of OH with n-hexane and 2,3-dimethyl-butane. The N-N-N estimation reproduces the experimental data fairly well for 2,3-dimethyl-butane (Fig. 9) and n-hexane (Fig. 4) at high temperatures. The N-N-N method could not be applied to the other five molecules studied here as the necessary site-specific H-abstraction rates are not available from Sivaramakrishnan and Michael [1,2].

According to N-N-N estimation method, the rate constant of 2,2-dimethyl-butane with OH can be decomposed to the various primary and secondary site-specific rate constants, as follows:

$$k_4 = 9P_3 + 2S_{30} + 3P_1 \quad (8)$$

where P_3 and P_1 have been determined by Sivaramakrishnan and Michael [1,2]. However, S_{30} is missing and hence the rate constant k_4 cannot be estimated using this method. However, having the Arrhenius expression of k_4 (Eq. (4)) from this work allows us to determine S_{30} which is expressed as follows,

$$\mathrm{S_{30}} = 2.374 \times 10^{-11}\exp(-1850\ \mathrm{K/T})\ \mathrm{cm^3\ molecule^{-1}\ s^{-1}}\ (887\text{–}1327\ \mathrm{K}) \quad (9)$$

Following the same methodology, rate constants for reactions R2, R3, R6, and R7 can be written in terms of the site-specific H-abstraction rates as:

$$k_2 = 6P_2 + T_{100} + 2S_{21} + 2S_{10} + 3P_1 \quad (10)$$

$$k_3 = 6P_1 + T_{101} + 4S_{20} + 3P_2 \quad (11)$$

$$k_6 = 6P_2 + T_{100} + 2S_{21} + 2S_{11'} + 2S_{11} + 2S_{10} + 3P_1 \quad (12)$$

$$k_7 = 6P_1 + 4S_{10} + 4S_{21} + T_{101} + 3P_2 \quad (13)$$

The rate expressions for T_{100}, S_{21}, T_{101}, and S_{20} are not available, whereas the other site-specific abstraction rates are given in [1]. In order to solve the above equations for the unknown rate constants, one site-specific rate has to be estimated to evaluate the others. By investigating the previously determined site-specific rates, we decided to estimate S_{20} because a clear trend can be established among S_{10} (Sivaramakrishnan and Michael [1]), S_{30} (current work), and the estimated S_{20} rate, as can be seen in Fig. 10. The S_{20} rate is estimated to be the average of the known S_{10} and S_{30} rates and has the following resulting expression:

$$\mathrm{S_{20}} = 1.58 \times 10^{-11}\exp(-1550\ \mathrm{K/T})\ \mathrm{cm^3\ molecule^{-1}\ s^{-1}}\ (887\text{–}1327\ \mathrm{K}) \quad (14)$$

Please cite this article in press as: J. Badra et al., *Proc. Combust. Inst.* (2014), http://dx.doi.org/10.1016/j.proci.2014.05.098

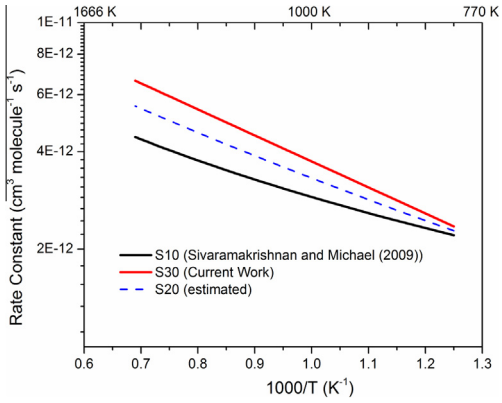

Fig. 10. Secondary site-specific H-abstraction rate constants.

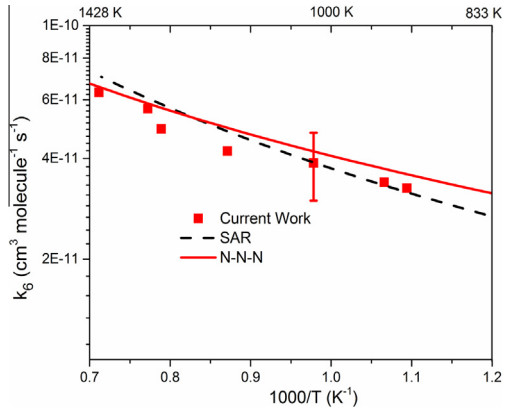

Fig. 11. Arrhenius plot of 2-methyl-heptane + OH ⇒ products.

Once S_{20} is evaluated, T_{101} rate can be calculated from measured k_3 and Eq. (11) and has the following expression:

$$T_{101} = 7.162 \times 10^{-12}\exp(-993\ \mathrm{K/T})\ \mathrm{cm^3\ molecule^{-1}\ s^{-1}}\ (883\text{–}1362\ \mathrm{K}) \quad (15)$$

Having the measured Arrhenius expression of k_7, the S_{21} rate is calculated to be:

$$S_{21} = 4.5 \times 10^{-12}\exp(-793.66\ \mathrm{K/T})\ \mathrm{cm^3\ molecule^{-1}\ s^{-1}}\ (833\text{–}1440\ \mathrm{K}) \quad (16)$$

After deriving the expression for S_{21}, T_{100} can now be calculated from measured k_2. The resulting Arrhenius expression is:

$$T_{100} = 2.85 \times 10^{-11}\exp(-1138.3\ \mathrm{K/T})\ \mathrm{cm^3\ molecule^{-1}\ s^{-1}}\ (878\text{–}1375\ \mathrm{K}) \quad (17)$$

The newly determined site-specific rate constants for H abstraction by OH are listed in Table 1. Having these site-specific rate constants as well as the rates from Sivaramakrishnan and Michael [1], rate constants of OH reaction with all n-alkanes, singly-methylated alkanes, and doubly-methylated alkanes can be estimated using the N-N-N method. As an example, the rate constant of OH + 2-methyl-heptane can now be estimated using the N-N-N method and compared with the measured data from the current work. The experimental rate constants of OH + 2-methyl-heptane as well as the SAR and N-N-N estimation methods are presented in Fig. 11. Both methods do a reasonable job of predicting the measured rate constants. The N-N-N estimation method is within 10–15% of our measured high temperature data. The agreement can perhaps be improved by extending the rate constant fits to lower temperatures and including the non-Arrhenius behavior expected for these rates. The determined site-specific rate constants can thus be extended to lower temperatures by combining the current high temperature measurements with low temperature data from literature. The rate constants can then be described with the modified Arrhenius expressions ($AT^b exp^{(-E/T)}$) and will be applicable over a much wider temperature range. However, this is beyond the scope of the current work and will be pursued in a separate study.

Table 1
Summary of H-abstraction by OH site-specific rate constants determined in this work. The rates are fit to Arrhenius expression A $\exp^{(-E/T)}$cm^3 molecule^{-1} s^{-1} and are applicable over 833–1440 K.

Group	A (cm^3 molecule^{-1} s^{-1})	E (K)
S_{20}	1.58×10^{-11}	1550
S_{30}	2.347×10^{-11}	1850
S_{21}	4.50×10^{-12}	794
T_{100}	2.85×10^{-11}	1138
T_{101}	7.962×10^{-12}	993

4. Summary

The rate constants for the reaction of seven alkanes with OH are measured behind reflected shock waves. The current measurements for n-hexane and 2,3-dimethyl-butane improve the previous determinations because of low scatter and small uncertainty. This work presents, to our knowledge, the first high-temperature rate constant measurements for five large alkanes; 2-methyl-pentane, 3-methyl-pentane, 2,2-dimethyl-butane, 2-methyl-heptane, and 4-methyl-heptane. Using these measurements we have derived new site-specific rate constants for H-abstraction from alkanes by OH radicals. These determinations enable the calculation of fuel + OH rate constants and branching ratios for all normal, singly-methylated, and doubly-methylated alkanes.

Please cite this article in press as: J. Badra et al., *Proc. Combust. Inst.* (2014), http://dx.doi.org/10.1016/j.proci.2014.05.098

Acknowledgements

We would like to acknowledge the funding support from Saudi Aramco under the FUELCOM program and by the Clean Combustion Research Center (CCRC) at King Abdullah University of Science and Technology (KAUST).

Appendix A. Supplementary material

Supplementary data associated with this article can be found, in the online version, at http://dx.doi.org/10.1016/j.proci.2014.05.098.

References

[1] R. Sivaramakrishnan, J.V. Michael, *J. Phys. Chem. A* 113 (17) (2009) 5047–5060.
[2] R. Sivaramakrishnan, N.K. Srinivasan, M.C. Su, J.V. Michael, *Proc. Combust. Inst.* 32 (1) (2009) 107–114.
[3] R. Atkinson, *Atmos. Chem. Phys.* 3 (6) (2003) 2233–2307.
[4] J.F. Bott, N. Cohen, *Int. J. Chem. Kinet.* 23 (12) (1991) 1075–1094.
[5] M. Colket, T. Edwards, S. Williams, N.P. Cernansky, D.L. Miller, F.L. Egolfopoulos, P. Lindstedt, K. Seshadri, F.L. Dryer, C.K. Law, D.G. Friend, D.B. Lenhert, H. Pitsch, A. Sarofim, M. Smooke, W. Tsang Development of an Experimental Database and Kinetic Models for Surrogate Jet Fuels, AIAA Technical Paper AIAA-2007-0770, Reston, VA, 2007, 2007.
[6] W.J. Pitz, N.P. Cernansky, F.L. Dryer, F.N. Egolfopoulos, J.T. Farrell, D.G. Friend, H. Pitsch Development of an Experimental Database and Chemical Kinetic Models for Surrogate Gasoline Fuels, SAE Technical Paper, Warrendale, PA, 2007.
[7] J.T. Farrell, N.P. Cernansky, F.L. Dryer, C.K. Law, D.G. Friend, C.A. Hergart, R.M. McDavid, A.K. Patel, C.J. Meuller, H. Pitsch, Development of an Experimental Database and Kinetic Models for Surrogate Diesel Fuels, SAE Technical Paper 2007-01-0201, Warrendale, PA, 2007, 2007.
[8] R. Atkinson, *Chem. Rev.* 86 (1) (1986) 69–201.
[9] R. Atkinson, *Kinetics and Mechanisms of the Gas-Phase Reactions of the Hydroxyl Radical with Organic Compounds*, American Chemical Society, Washington, DC and New York, NY, 1989, pp. 1–246.
[10] R. Atkinson, *Atmos. Environ.. Part A. Gen. Top.* 24 (1) (1990) 1–41.
[11] R. Atkinson, *J. Phys. Chem. Ref. Data* 26 (2) (1997) 215–290.
[12] A.T. Droege, F.P. Tully, *J. Phys. Chem.* 90 (9) (1986) 1949–1954.
[13] A.T. Droege, F.P. Tully, *J. Phys. Chem.* 91 (5) (1987) 1222–1225.
[14] A.T. Droege, F.P. Tully, *J. Phys. Chem.* 90 (22) (1986) 5937–5941.
[15] F.P. Tully, A.T. Droege, M.L. Koszykowski, C.F. Melius, *J. Phys. Chem.* 90 (4) (1986) 691–698.
[16] F.P. Tully, J.E.M. Goldsmith, A.T. Droege, *J. Phys. Chem.* 90 (22) (1986) 5932–5937.
[17] F.P. Tully, M.L. Koszykowski, J. Stephen Binkley, *Proc. Combust. Inst.* 20 (1) (1985) 715–721.
[18] J.F. Bott, N. Cohen, *Int. J. Chem. Kinet.* 23 (1991) 1017–1033.
[19] J.F. Bott, N. Cohen, *Int. J. Chem. Kinet.* 16 (12) (1984) 1557–1566.
[20] J.F. Bott, N. Cohen, *Int. J. Chem. Kinet.* 21 (7) (1989) 485–498.
[21] J.B. Koffend, N. Cohen, *Int. J. Chem. Kinet.* 28 (2) (1996) 79–87.
[22] G.A. Pang, R.K. Hanson, D.M. Golden, C.T. Bowman, *PCCP* 225 (11–12) (2011) 1157–1178.
[23] N. Cohen, *Int. J. Chem. Kinet.* 14 (12) (1982) 1339–1362.
[24] N. Cohen, *Int. J. Chem. Kinet.* 23 (5) (1991) 397–417.
[25] E.S.C. Kwok, R. Atkinson, *Atmos. Environ.* 29 (14) (1995) 1685–1695.
[26] J. Badra, A. Elwardany, F. Khaled, S.S. Vasu, A. Farooq, *Combust. Flame* 161 (3) (2014) 725–734.
[27] J. Badra, A. Elwardany, A. Farooq, *PCCP* 16 (24) (2014) 12183–12193.
[28] J.T. Herbon, R.K. Hanson, D.M. Golden, C.T. Bowman, *Proc. Combust. Inst.* 29 (1) (2002) 1201–1208.
[29] K. Lam, D. Davidson, R. Hanson, *J. Phys. Chem. A* 116 (2012) 5549–5559.
[30] V. Vasudevan, D.F. Davidson, R.K. Hanson, *J. Phys. Chem. A* 109 (2005) 3352–3359.
[31] Z. Hong, S.S. Vasu, D.F. Davidson, R.K. Hanson, *J. Phys. Chem. A* 114 (17) (2010) 5520–5525.
[32] G.A. Pang, R.K. Hanson, D.M. Golden, C.T. Bowman, *J. Phys. Chem. A* 116 (10) (2012) 2475–2483.
[33] G.A. Pang, R.K. Hanson, D.M. Golden, C.T. Bowman, *J. Phys. Chem. A* 116 (19) (2012) 4720–4725.
[34] S.S. Vasu, D.F. Davidson, R.K. Hanson, D.M. Golden, *Chem. Phys. Lett.* 497 (1–3) (2010) 26–29.
[35] S.S. Vasu, Z. Hong, D.F. Davidson, R.K. Hanson, D.M. Golden, *J. Phys. Chem. A* 114 (43) (2010) 11529–11537.
[36] R. Design, in: 15112 ed.; Reaction Design: San Diego, 2011.
[37] S.M. Sarathy, C.K. Westbrook, M. Mehl, W.J. Pitz, C. Togbe, P. Dagaut, H. Wang, M.A. Oehlschlaeger, U. Niemann, K. Seshadri, P.S. Veloo, C. Ji, F.N. Egolfopoulos, T. Lu, *Combust. Flame* 158 (12) (2011) 2338–2357.